

Measurements of branching fraction and final-state asymmetry of the $\bar{B}^0(B^0) \rightarrow K_S^0 K^\mp \pi^\pm$ decay at Belle

A. Abdesselam,¹⁰⁰ I. Adachi,^{22, 18} K. Adamczyk,⁷⁴ J. K. Ahn,⁴⁹ H. Aihara,¹⁰⁸
S. Al Said,^{100, 47} K. Arinstein,^{5, 78} Y. Arita,⁶⁶ D. M. Asner,⁴ H. Atmacan,⁹⁶
V. Aulchenko,^{5, 78} T. Aushev,⁶⁵ R. Ayad,¹⁰⁰ T. Aziz,¹⁰¹ V. Babu,¹⁰¹ I. Badhrees,^{100, 46}
S. Bahinipati,²⁹ A. M. Bakich,⁹⁹ Y. Ban,⁸³ V. Bansal,⁸¹ E. Barberio,⁶¹ M. Barrett,¹¹⁴
W. Bartel,¹⁰ P. Behera,³² C. Beleño,¹⁷ K. Belous,³⁶ M. Berger,⁹⁷ F. Bernlochner,³
D. Besson,⁶⁴ V. Bhardwaj,²⁸ B. Bhuyan,³⁰ T. Bilka,⁶ J. Biswal,⁴¹ T. Bloomfield,⁶¹
A. Bobrov,^{5, 78} A. Bondar,^{5, 78} G. Bonvicini,¹¹⁴ A. Bozek,⁷⁴ M. Bračko,^{59, 41} N. Braun,⁴³
F. Breibeck,³⁵ J. Brodzicka,⁷⁴ T. E. Browder,²¹ L. Cao,⁴³ G. Caria,⁶¹ D. Červenkov,⁶
M.-C. Chang,¹³ P. Chang,⁷³ Y. Chao,⁷³ V. Chekelian,⁶⁰ A. Chen,⁷¹ K.-F. Chen,⁷³
B. G. Cheon,²⁰ K. Chilikin,⁵⁴ R. Chistov,^{54, 64} K. Cho,⁴⁸ V. Chobanova,⁶⁰ S.-K. Choi,¹⁹
Y. Choi,⁹⁸ S. Choudhury,³¹ D. Cinabro,¹¹⁴ J. Crnkovic,²⁷ S. Cunliffe,¹⁰ T. Czank,¹⁰⁶
M. Danilov,^{64, 54} N. Dash,²⁹ S. Di Carlo,⁵² J. Dingfelder,³ Z. Doležal,⁶ T. V. Dong,^{22, 18}
D. Dossett,⁶¹ Z. Drásal,⁶ A. Drutskoy,^{54, 64} S. Dubey,²¹ D. Dutta,¹⁰¹ S. Eidelman,^{5, 78}
D. Epifanov,^{5, 78} J. E. Fast,⁸¹ M. Feindt,⁴³ T. Ferber,¹⁰ A. Frey,¹⁷ O. Frost,¹⁰
B. G. Fulsom,⁸¹ R. Garg,⁸² V. Gaur,¹⁰¹ N. Gabyshev,^{5, 78} A. Garmash,^{5, 78} M. Gelb,⁴³
J. Gemmler,⁴³ D. Getzkow,¹⁵ F. Giordano,²⁷ A. Giri,³¹ R. Glattauer,³⁵ Y. M. Goh,²⁰
P. Goldenzweig,⁴³ B. Golob,^{55, 41} D. Greenwald,¹⁰³ M. Grosse Perdekamp,^{27, 89} J. Grygier,⁴³
O. Grzymkowska,⁷⁴ Y. Guan,^{33, 22} E. Guido,³⁹ H. Guo,⁹¹ J. Haba,^{22, 18} P. Hamer,¹⁷
K. Hara,²² T. Hara,^{22, 18} Y. Hasegawa,⁹³ J. Hasenbusch,³ K. Hayasaka,⁷⁶ H. Hayashii,⁷⁰
X. H. He,⁸³ M. Heck,⁴³ M. T. Hedges,²¹ D. Heffernan,⁸⁰ M. Heider,⁴³ A. Heller,⁴³
T. Higuchi,⁴⁴ S. Hirose,⁶⁶ T. Horiguchi,¹⁰⁶ Y. Hoshi,¹⁰⁵ K. Hoshina,¹¹¹ W.-S. Hou,⁷³
Y. B. Hsiung,⁷³ C.-L. Hsu,⁹⁹ K. Huang,⁷³ M. Huschle,⁴³ Y. Igarashi,²² T. Iijima,^{67, 66}
M. Imamura,⁶⁶ K. Inami,⁶⁶ G. Inguglia,¹⁰ A. Ishikawa,¹⁰⁶ K. Itagaki,¹⁰⁶ R. Itoh,^{22, 18}
M. Iwasaki,⁷⁹ Y. Iwasaki,²² S. Iwata,¹¹⁰ W. W. Jacobs,³³ I. Jaegle,¹² H. B. Jeon,⁵¹ S. Jia,²
Y. Jin,¹⁰⁸ D. Joffe,⁴⁵ M. Jones,²¹ K. K. Joo,⁸ T. Julius,⁶¹ J. Kahn,⁵⁶ H. Kakuno,¹¹⁰
A. B. Kaliyar,³² J. H. Kang,¹¹⁶ K. H. Kang,⁵¹ P. Kapusta,⁷⁴ G. Karyan,¹⁰ S. U. Kataoka,⁶⁹
E. Kato,¹⁰⁶ Y. Kato,⁶⁶ P. Katrenko,^{65, 54} H. Kawai,⁷ T. Kawasaki,⁷⁶ T. Keck,⁴³
H. Kichimi,²² C. Kiesling,⁶⁰ B. H. Kim,⁹² D. Y. Kim,⁹⁵ H. J. Kim,⁵¹ H.-J. Kim,¹¹⁶
J. B. Kim,⁴⁹ K. T. Kim,⁴⁹ S. H. Kim,²⁰ S. K. Kim,⁹² Y. J. Kim,⁴⁹ T. Kimmel,¹¹³
H. Kindo,^{22, 18} K. Kinoshita,⁹ C. Kleinwort,¹⁰ J. Klucar,⁴¹ N. Kobayashi,¹⁰⁹ P. Kodyš,⁶
Y. Koga,⁶⁶ T. Konno,¹¹⁷ S. Korpar,^{59, 41} D. Kotchetkov,²¹ R. T. Kouzes,⁸¹ P. Križan,^{55, 41}
R. Kroeger,⁶² J.-F. Krohn,⁶¹ P. Krokovny,^{5, 78} B. Kronenbitter,⁴³ T. Kuhr,⁵⁶ R. Kulasiri,⁴⁵
R. Kumar,⁸⁵ T. Kumita,¹¹⁰ E. Kurihara,⁷ Y. Kuroki,⁸⁰ A. Kuzmin,^{5, 78} P. Kvasnička,⁶
Y.-J. Kwon,¹¹⁶ Y.-T. Lai,²² J. S. Lange,¹⁵ I. S. Lee,²⁰ S. C. Lee,⁵¹ M. Leitgab,^{27, 89}
R. Leitner,⁶ D. Levit,¹⁰³ P. Lewis,²¹ C. H. Li,⁶¹ H. Li,³³ L. K. Li,³⁴ Y. Li,¹¹³ Y. B. Li,⁸³
L. Li Gioi,⁶⁰ J. Libby,³² A. Limosani,⁶¹ C. Liu,⁹¹ Y. Liu,⁹ D. Liventsev,^{113, 22} A. Loos,⁹⁶
R. Louvot,⁵³ P.-C. Lu,⁷³ M. Lubej,⁴¹ T. Luo,¹⁴ J. MacNaughton,⁶³ M. Masuda,¹⁰⁷
T. Matsuda,⁶³ D. Matvienko,^{5, 78} A. Matyja,⁷⁴ J. T. McNeil,¹² M. Merola,^{38, 68} F. Metzner,⁴³
Y. Mikami,¹⁰⁶ K. Miyabayashi,⁷⁰ Y. Miyachi,¹¹⁵ H. Miyake,^{22, 18} H. Miyata,⁷⁶ Y. Miyazaki,⁶⁶

R. Mizuk,^{54, 64, 65} G. B. Mohanty,¹⁰¹ S. Mohanty,^{101, 112} H. K. Moon,⁴⁹ T. Mori,⁶⁶
T. Morii,⁴⁴ H.-G. Moser,⁶⁰ M. Mrvar,⁴¹ T. Müller,⁴³ N. Muramatsu,⁸⁶ R. Mussa,³⁹
Y. Nagasaka,²⁵ Y. Nakahama,¹⁰⁸ I. Nakamura,^{22, 18} K. R. Nakamura,²² E. Nakano,⁷⁹
H. Nakano,¹⁰⁶ T. Nakano,⁸⁷ M. Nakao,^{22, 18} H. Nakayama,^{22, 18} H. Nakazawa,⁷³ T. Nanut,⁴¹
K. J. Nath,³⁰ Z. Natkaniec,⁷⁴ M. Nayak,^{114, 22} K. Neichi,¹⁰⁵ C. Ng,¹⁰⁸ C. Niebuhr,¹⁰
M. Niiyama,⁵⁰ N. K. Nisar,⁸⁴ S. Nishida,^{22, 18} K. Nishimura,²¹ O. Nitoh,¹¹¹ A. Ogawa,⁸⁹
K. Ogawa,⁷⁶ S. Ogawa,¹⁰⁴ T. Ohshima,⁶⁶ S. Okuno,⁴² S. L. Olsen,¹⁹ H. Ono,^{75, 76}
Y. Ono,¹⁰⁶ Y. Onuki,¹⁰⁸ W. Ostrowicz,⁷⁴ C. Oswald,³ H. Ozaki,^{22, 18} P. Pakhlov,^{54, 64}
G. Pakhlova,^{54, 65} B. Pal,⁴ H. Palka,⁷⁴ E. Panzenböck,^{17, 70} S. Pardi,³⁸ C.-S. Park,¹¹⁶
C. W. Park,⁹⁸ H. Park,⁵¹ K. S. Park,⁹⁸ S. Paul,¹⁰³ I. Pavelkin,⁶⁵ T. K. Pedlar,⁵⁷ T. Peng,⁹¹
L. Pesántez,³ R. Pestotnik,⁴¹ M. Peters,²¹ L. E. Piilonen,¹¹³ A. Poluektov,^{5, 78}
V. Popov,^{54, 65} K. Prasanth,¹⁰¹ E. Prencipe,²⁴ M. Prim,⁴³ K. Prothmann,^{60, 102}
M. V. Purohit,⁹⁶ A. Rabusov,¹⁰³ J. Rauch,¹⁰³ B. Reisert,⁶⁰ P. K. Resmi,³² E. Ríbežl,⁴¹
M. Ritter,⁵⁶ J. Rorie,²¹ A. Rostomyan,¹⁰ M. Rozanska,⁷⁴ S. Rummel,⁵⁶ G. Russo,³⁸
D. Sahoo,¹⁰¹ H. Sahoo,⁶² T. Saito,¹⁰⁶ Y. Sakai,^{22, 18} M. Salehi,^{58, 56} S. Sandilya,⁹ D. Santel,⁹
L. Santelj,²² T. Sanuki,¹⁰⁶ J. Sasaki,¹⁰⁸ N. Sasao,⁵⁰ Y. Sato,⁶⁶ V. Savinov,⁸⁴ T. Schlüter,⁵⁶
O. Schneider,⁵³ G. Schnell,^{1, 26} P. Schönmeier,¹⁰⁶ M. Schram,⁸¹ C. Schwanda,³⁵
A. J. Schwartz,⁹ B. Schwenker,¹⁷ R. Seidl,⁸⁹ Y. Seino,⁷⁶ D. Semmler,¹⁵ K. Senyo,¹¹⁵
O. Seon,⁶⁶ I. S. Seong,²¹ M. E. Seviour,⁶¹ L. Shang,³⁴ M. Shapkin,³⁶ V. Shebalin,^{5, 78}
C. P. Shen,² T.-A. Shibata,¹⁰⁹ H. Shibuya,¹⁰⁴ S. Shinomiya,⁸⁰ J.-G. Shiu,⁷³ B. Shwartz,^{5, 78}
A. Sibidanov,⁹⁹ F. Simon,^{60, 102} J. B. Singh,⁸² R. Sinha,³⁷ A. Sokolov,³⁶ Y. Soloviev,¹⁰
E. Solovieva,^{54, 65} S. Stanič,⁷⁷ M. Starič,⁴¹ M. Steder,¹⁰ Z. Stottler,¹¹³ J. F. Strube,⁸¹
J. Stypula,⁷⁴ S. Sugihara,¹⁰⁸ A. Sugiyama,⁹⁰ M. Sumihama,¹⁶ K. Sumisawa,^{22, 18}
T. Sumiyoshi,¹¹⁰ W. Sutcliffe,⁴³ K. Suzuki,⁶⁶ K. Suzuki,⁹⁷ S. Suzuki,⁹⁰ S. Y. Suzuki,²²
Z. Suzuki,¹⁰⁶ H. Takeichi,⁶⁶ M. Takizawa,^{94, 23, 88} U. Tamponi,³⁹ M. Tanaka,^{22, 18}
S. Tanaka,^{22, 18} K. Tanida,⁴⁰ N. Taniguchi,²² Y. Tao,¹² G. N. Taylor,⁶¹ F. Tenchini,⁶¹
Y. Teramoto,⁷⁹ I. Tikhomirov,⁶⁴ K. Trabelsi,^{22, 18} T. Tsuboyama,^{22, 18} M. Uchida,¹⁰⁹
T. Uchida,²² I. Ueda,²² S. Uehara,^{22, 18} T. Uglov,^{54, 65} Y. Unno,²⁰ S. Uno,^{22, 18} P. Urquijo,⁶¹
Y. Ushiroda,^{22, 18} Y. Usov,^{5, 78} S. E. Vahsen,²¹ R. Van Tonder,⁴³ C. Van Hulse,¹
P. Vanhoefer,⁶⁰ G. Varner,²¹ K. E. Varvell,⁹⁹ K. Vervink,⁵³ A. Vinokurova,^{5, 78}
V. Vorobyev,^{5, 78} A. Vossen,¹¹ M. N. Wagner,¹⁵ E. Waheed,⁶¹ B. Wang,⁹ C. H. Wang,⁷²
M.-Z. Wang,⁷³ P. Wang,³⁴ X. L. Wang,¹⁴ M. Watanabe,⁷⁶ Y. Watanabe,⁴² S. Watanuki,¹⁰⁶
R. Wedd,⁶¹ S. Wehle,¹⁰ E. Widmann,⁹⁷ J. Wiechczynski,⁷⁴ K. M. Williams,¹¹³
E. Won,⁴⁹ B. D. Yabsley,⁹⁹ S. Yamada,²² H. Yamamoto,¹⁰⁶ Y. Yamashita,⁷⁵
S. Yashchenko,¹⁰ H. Ye,¹⁰ J. Yelton,¹² J. H. Yin,³⁴ Y. Yook,¹¹⁶ C. Z. Yuan,³⁴ Y. Yusa,⁷⁶
S. Zakharov,^{54, 65} C. C. Zhang,³⁴ L. M. Zhang,⁹¹ Z. P. Zhang,⁹¹ L. Zhao,⁹¹ V. Zhilich,^{5, 78}
V. Zhukova,^{54, 64} V. Zhulanov,^{5, 78} T. Zivko,⁴¹ A. Zupanc,^{55, 41} and N. Zwahlen⁵³

(The Belle Collaboration)

¹University of the Basque Country UPV/EHU, 48080 Bilbao

²Beihang University, Beijing 100191

³University of Bonn, 53115 Bonn

⁴Brookhaven National Laboratory, Upton, New York 11973

⁵Budker Institute of Nuclear Physics SB RAS, Novosibirsk 630090

⁶Faculty of Mathematics and Physics, Charles University, 121 16 Prague

- ⁷*Chiba University, Chiba 263-8522*
- ⁸*Chonnam National University, Kwangju 660-701*
- ⁹*University of Cincinnati, Cincinnati, Ohio 45221*
- ¹⁰*Deutsches Elektronen-Synchrotron, 22607 Hamburg*
- ¹¹*Duke University, Durham, North Carolina 27708*
- ¹²*University of Florida, Gainesville, Florida 32611*
- ¹³*Department of Physics, Fu Jen Catholic University, Taipei 24205*
- ¹⁴*Key Laboratory of Nuclear Physics and Ion-beam Application (MOE) and Institute of Modern Physics, Fudan University, Shanghai 200443*
- ¹⁵*Justus-Liebig-Universität Gießen, 35392 Gießen*
- ¹⁶*Gifu University, Gifu 501-1193*
- ¹⁷*II. Physikalisches Institut, Georg-August-Universität Göttingen, 37073 Göttingen*
- ¹⁸*SOKENDAI (The Graduate University for Advanced Studies), Hayama 240-0193*
- ¹⁹*Gyeongsang National University, Chinju 660-701*
- ²⁰*Hanyang University, Seoul 133-791*
- ²¹*University of Hawaii, Honolulu, Hawaii 96822*
- ²²*High Energy Accelerator Research Organization (KEK), Tsukuba 305-0801*
- ²³*J-PARC Branch, KEK Theory Center, High Energy Accelerator Research Organization (KEK), Tsukuba 305-0801*
- ²⁴*Forschungszentrum Jülich, 52425 Jülich*
- ²⁵*Hiroshima Institute of Technology, Hiroshima 731-5193*
- ²⁶*IKERBASQUE, Basque Foundation for Science, 48013 Bilbao*
- ²⁷*University of Illinois at Urbana-Champaign, Urbana, Illinois 61801*
- ²⁸*Indian Institute of Science Education and Research Mohali, SAS Nagar, 140306*
- ²⁹*Indian Institute of Technology Bhubaneswar, Satya Nagar 751007*
- ³⁰*Indian Institute of Technology Guwahati, Assam 781039*
- ³¹*Indian Institute of Technology Hyderabad, Telangana 502285*
- ³²*Indian Institute of Technology Madras, Chennai 600036*
- ³³*Indiana University, Bloomington, Indiana 47408*
- ³⁴*Institute of High Energy Physics, Chinese Academy of Sciences, Beijing 100049*
- ³⁵*Institute of High Energy Physics, Vienna 1050*
- ³⁶*Institute for High Energy Physics, Protvino 142281*
- ³⁷*Institute of Mathematical Sciences, Chennai 600113*
- ³⁸*INFN - Sezione di Napoli, 80126 Napoli*
- ³⁹*INFN - Sezione di Torino, 10125 Torino*
- ⁴⁰*Advanced Science Research Center, Japan Atomic Energy Agency, Naka 319-1195*
- ⁴¹*J. Stefan Institute, 1000 Ljubljana*
- ⁴²*Kanagawa University, Yokohama 221-8686*
- ⁴³*Institut für Experimentelle Teilchenphysik, Karlsruher Institut für Technologie, 76131 Karlsruhe*
- ⁴⁴*Kavli Institute for the Physics and Mathematics of the Universe (WPI), University of Tokyo, Kashiwa 277-8583*
- ⁴⁵*Kennesaw State University, Kennesaw, Georgia 30144*
- ⁴⁶*King Abdulaziz City for Science and Technology, Riyadh 11442*

- ⁴⁷*Department of Physics, Faculty of Science,
King Abdulaziz University, Jeddah 21589*
- ⁴⁸*Korea Institute of Science and Technology Information, Daejeon 305-806*
- ⁴⁹*Korea University, Seoul 136-713*
- ⁵⁰*Kyoto University, Kyoto 606-8502*
- ⁵¹*Kyungpook National University, Daegu 702-701*
- ⁵²*LAL, Univ. Paris-Sud, CNRS/IN2P3, Université Paris-Saclay, Orsay*
- ⁵³*École Polytechnique Fédérale de Lausanne (EPFL), Lausanne 1015*
- ⁵⁴*P.N. Lebedev Physical Institute of the Russian Academy of Sciences, Moscow 119991*
- ⁵⁵*Faculty of Mathematics and Physics,
University of Ljubljana, 1000 Ljubljana*
- ⁵⁶*Ludwig Maximilians University, 80539 Munich*
- ⁵⁷*Luther College, Decorah, Iowa 52101*
- ⁵⁸*University of Malaya, 50603 Kuala Lumpur*
- ⁵⁹*University of Maribor, 2000 Maribor*
- ⁶⁰*Max-Planck-Institut für Physik, 80805 München*
- ⁶¹*School of Physics, University of Melbourne, Victoria 3010*
- ⁶²*University of Mississippi, University, Mississippi 38677*
- ⁶³*University of Miyazaki, Miyazaki 889-2192*
- ⁶⁴*Moscow Physical Engineering Institute, Moscow 115409*
- ⁶⁵*Moscow Institute of Physics and Technology, Moscow Region 141700*
- ⁶⁶*Graduate School of Science, Nagoya University, Nagoya 464-8602*
- ⁶⁷*Kobayashi-Maskawa Institute, Nagoya University, Nagoya 464-8602*
- ⁶⁸*Università di Napoli Federico II, 80055 Napoli*
- ⁶⁹*Nara University of Education, Nara 630-8528*
- ⁷⁰*Nara Women's University, Nara 630-8506*
- ⁷¹*National Central University, Chung-li 32054*
- ⁷²*National United University, Miao Li 36003*
- ⁷³*Department of Physics, National Taiwan University, Taipei 10617*
- ⁷⁴*H. Niewodniczanski Institute of Nuclear Physics, Krakow 31-342*
- ⁷⁵*Nippon Dental University, Niigata 951-8580*
- ⁷⁶*Niigata University, Niigata 950-2181*
- ⁷⁷*University of Nova Gorica, 5000 Nova Gorica*
- ⁷⁸*Novosibirsk State University, Novosibirsk 630090*
- ⁷⁹*Osaka City University, Osaka 558-8585*
- ⁸⁰*Osaka University, Osaka 565-0871*
- ⁸¹*Pacific Northwest National Laboratory, Richland, Washington 99352*
- ⁸²*Panjab University, Chandigarh 160014*
- ⁸³*Peking University, Beijing 100871*
- ⁸⁴*University of Pittsburgh, Pittsburgh, Pennsylvania 15260*
- ⁸⁵*Punjab Agricultural University, Ludhiana 141004*
- ⁸⁶*Research Center for Electron Photon Science,
Tohoku University, Sendai 980-8578*
- ⁸⁷*Research Center for Nuclear Physics, Osaka University, Osaka 567-0047*
- ⁸⁸*Theoretical Research Division, Nishina Center, RIKEN, Saitama 351-0198*
- ⁸⁹*RIKEN BNL Research Center, Upton, New York 11973*
- ⁹⁰*Saga University, Saga 840-8502*

- ⁹¹*University of Science and Technology of China, Hefei 230026*
⁹²*Seoul National University, Seoul 151-742*
⁹³*Shinshu University, Nagano 390-8621*
⁹⁴*Showa Pharmaceutical University, Tokyo 194-8543*
⁹⁵*Soongsil University, Seoul 156-743*
⁹⁶*University of South Carolina, Columbia, South Carolina 29208*
⁹⁷*Stefan Meyer Institute for Subatomic Physics, Vienna 1090*
⁹⁸*Sungkyunkwan University, Suwon 440-746*
⁹⁹*School of Physics, University of Sydney, New South Wales 2006*
¹⁰⁰*Department of Physics, Faculty of Science, University of Tabuk, Tabuk 71451*
¹⁰¹*Tata Institute of Fundamental Research, Mumbai 400005*
¹⁰²*Excellence Cluster Universe, Technische Universität München, 85748 Garching*
¹⁰³*Department of Physics, Technische Universität München, 85748 Garching*
¹⁰⁴*Toho University, Funabashi 274-8510*
¹⁰⁵*Tohoku Gakuin University, Tagajo 985-8537*
¹⁰⁶*Department of Physics, Tohoku University, Sendai 980-8578*
¹⁰⁷*Earthquake Research Institute, University of Tokyo, Tokyo 113-0032*
¹⁰⁸*Department of Physics, University of Tokyo, Tokyo 113-0033*
¹⁰⁹*Tokyo Institute of Technology, Tokyo 152-8550*
¹¹⁰*Tokyo Metropolitan University, Tokyo 192-0397*
¹¹¹*Tokyo University of Agriculture and Technology, Tokyo 184-8588*
¹¹²*Utkal University, Bhubaneswar 751004*
¹¹³*Virginia Polytechnic Institute and State University, Blacksburg, Virginia 24061*
¹¹⁴*Wayne State University, Detroit, Michigan 48202*
¹¹⁵*Yamagata University, Yamagata 990-8560*
¹¹⁶*Yonsei University, Seoul 120-749*
¹¹⁷*Kitasato University, Tokyo 108-0072*

Abstract

We report the measurement of the branching fraction and final-state asymmetry for the $\bar{B}^0(B^0) \rightarrow K_S^0 K^\mp \pi^\pm$ decays. The analysis is based on a data sample of 711 fb^{-1} collected at the $\Upsilon(4S)$ resonance with the Belle detector at the KEKB asymmetric-energy e^+e^- collider. We obtain a branching fraction of $(3.60 \pm 0.33 \pm 0.15) \times 10^{-6}$ and a final-state asymmetry of $(-8.5 \pm 8.9 \pm 0.2)\%$, where the first uncertainties are statistical and the second are systematic. Hints of peaking structures are observed in the differential branching fraction plotted as functions of Dalitz variables.

PACS numbers: 14.40.Nd, 13.20.Hw, 13.25.-k, 11.30.Er

Three-body charmless hadronic B decays are suppressed in the standard model (SM) and are also sensitive to localized CP violation in the phase space [1, 2]. The $\bar{B}^0(B^0) \rightarrow K_S^0 K^\mp \pi^\pm$ [3] decays with even number of kaons have a smaller decay rate compared to the cases with odd number of kaons. These proceed via the $b \rightarrow u$ tree-level, the $b \rightarrow u$ W -exchange, and the $b \rightarrow d$ penguin process with a virtual loop, which provides an opportunity to search for physics beyond the SM since new heavy particles may cause deviations from SM predictions.

Previous measurements by the BaBar [4, 5] and LHCb [6–8] experiments find hints of structures at the low $K^-\pi^+$ and $K^-K_S^0$ regions that have highly asymmetric helicity angular distributions. However, the yield is not enough to draw firm conclusions with a full Dalitz analysis. Similar studies on $B^+ \rightarrow K^+K^-\pi^+$ were performed by Belle [9], BaBar [10], and LHCb [11, 12], in which strong evidence of localized CP violation was found in the low $M_{K^+K^-}$ region.

By using the full data set of Belle, we expect to measure the branching fraction and final-state asymmetry of $\bar{B}^0(B^0) \rightarrow K_S^0 K^\mp \pi^\pm$ decays more precisely. Using charges of final-state particles, the latter is defined as

$$\mathcal{A} = \frac{N(K_S^0 K^- \pi^+) - N(K_S^0 K^+ \pi^-)}{N(K_S^0 K^- \pi^+) + N(K_S^0 K^+ \pi^-)}, \quad (1)$$

where N denotes the measured signal yield of the corresponding B final states. \mathcal{A} is distinct from the direct CP asymmetry; rather it is an asymmetry between the decay final states of $K^0 K^- \pi^+$ and $\bar{K}^0 K^+ \pi^-$ where $K^0(\bar{K}^0)$ leads to a K_S^0 . We measure \mathcal{A} as the measurement of direct CP asymmetry based on flavor tagging won't be so precise. Only about 30% of events can be effectively flavor-tagged, which would be further affected by B^0 - \bar{B}^0 mixing. In addition, we use the *sPlot* [13] method to obtain the background-subtracted yields for the Dalitz variables $M_{K^-\pi^+}$, $M_{\pi^+K_S^0}$, and $M_{K^-K_S^0}$, and hence determine their differential branching fractions. The total branching fraction is extracted by integrating the differential branching fraction.

Our measurements are obtained from a data sample of 711 fb^{-1} , corresponding to 772×10^6 $B\bar{B}$ pairs, collected with the Belle detector [14] operating at the KEKB asymmetric-energy e^+e^- collider [15]. The Belle detector is a large-solid-angle magnetic spectrometer that consists of a silicon vertex detector (SVD), a 50-layer central drift chamber (CDC), an array of aerogel threshold Cherenkov counters (ACC), a barrel-like arrangement of time-of-flight scintillation counters (TOF) and an electromagnetic calorimeter comprised of CsI(Tl) crystals, all located inside a superconducting solenoid that provides a 1.5 T magnetic field. An iron flux-return yoke located outside the solenoid is instrumented to detect K_L^0 mesons and muons. The detector is described in detail elsewhere [14].

This analysis uses the data sets with two different inner-detector configurations. About 140 fb^{-1} were collected with a beam-pipe of radius 2.0 cm and with 3 layers of SVD, while the rest of the data set was recorded with a beam-pipe of radius 1.5 cm and 4 layers of SVD [16]. Large samples Monte Carlo (MC) events for signal and backgrounds are generated with EvtGen [17] and subsequently simulated with GEANT3 [18] with the configurations of the Belle detector. These samples are used to obtain expected distributions of various physical quantities for signal and backgrounds, to optimize selection criteria as well as to determine the signal detection efficiency.

The selection criteria for the final-state charged particles in the $\bar{B}^0(B^0) \rightarrow K_S^0 K^\mp \pi^\pm$ reconstruction are based on information obtained from the tracking systems (SVD and

CDC) and the charged-hadron identification (PID) systems namely CDC, ACC, and TOF. The charged kaons and pions are required to have an impact parameter within ± 0.2 cm of the interaction point (IP) in the transverse plane, and within ± 5.0 cm along the e^+ beam direction. The likelihood values of each track for kaon and pion hypotheses (L_K and L_π) are determined from the information provided by the PID system. The track is identified as a kaon if $L_K/(L_K + L_\pi) > 0.6$ else as a pion. The efficiency for identifying a pion (kaon) is about 88% (86%), which depends on the momentum of the track, while the probability for a pion or a kaon to be misidentified as the other one is less than 10%. The efficiency and misidentification probability are averaged over the momentum of the final-state particles. The K_S^0 candidates are reconstructed via the $K_S^0 \rightarrow \pi^+\pi^-$ decay, and the identification is enhanced by using a neural network (NN) [19] which combines seven kinematic variables of K_S^0 [20]. The invariant mass of the K_S^0 candidates are required to be within ± 10 MeV/ c^2 of the world average, which corresponds to about three times of the resolution. The vertex fit of $K_S^0 \rightarrow \pi^+\pi^-$ is required to succeed with the goodness-of-fit value (χ^2) less than 20.

B mesons are identified with two kinematic variables calculated in the center-of-mass frame: the beam-energy-constrained-mass $M_{bc} \equiv \sqrt{E_{\text{beam}}^2/c^4 - |\vec{p}_B/c|^2}$, and the energy difference $\Delta E \equiv E_B - E_{\text{beam}}$, where E_{beam} is the beam energy, and \vec{p}_B (E_B) is the momentum (energy) of the reconstructed B meson. The B candidates are required to have $M_{bc} > 5.255$ GeV/ c^2 and $|\Delta E| < 0.15$ GeV, and the signal region is defined as 5.272 GeV/ $c^2 < M_{bc} < 5.288$ GeV/ c^2 and $|\Delta E| < 0.05$ GeV. We require a vertex fit for $\bar{B}^0(B^0) \rightarrow K_S^0 K^\mp \pi^\pm$ candidates with $\chi^2 < 100$. We find that 9% of events have more than one B candidates. In those cases, we choose the one with the smallest χ^2 value. Our best B selection method chooses the correct candidate in 99% of cases.

The dominant background arises from the continuum $e^+e^- \rightarrow q\bar{q}$ ($q = u, d, s, c$) process. To suppress this, we construct a Fisher discriminant [21] from 17 modified Fox-Wolfram moments [22]. To further improve the distinguishing power, we combine the output of the Fisher discriminant with four more variables in a NN. These are: the cosine of the angle between the reconstructed B flight direction and the beam direction in the CM frame, the offset between the vertex of the reconstructed B and that of the rest of the tracks' vertex along the z axis, the cosine of the angle between the thrust axis [23] of the reconstructed B and that of the rest of the event in the CM frame, and a B meson flavor tagging quality variable. The NN is trained with signal and continuum MC samples. The NN output (C_{NN}) ranges from -1 to 1 , and it is required to be greater than 0.7 . This removes 93% of continuum background while 82% of the signal is retained. We transform C_{NN} to $C'_{\text{NN}} \equiv \log\left(\frac{C_{\text{NN}} - C_{\text{NN}}^{\min}}{C_{\text{NN}}^{\max} - C_{\text{NN}}}\right)$, where C_{NN}^{\min} is 0.7 and C_{NN}^{\max} is the maximum value of C_{NN} .

Background events from B decays mediated via the $b \rightarrow c$ transition (generic B decays) exhibit peaking structures in the signal region. They are mainly due to the two-body decays of D mesons and J/ψ , e.g., $D^0 \rightarrow K^-\pi^+$, $D^- \rightarrow K^-K_S^0$, $D_s^- \rightarrow K^-K_S^0$, $J/\psi \rightarrow e^+e^-$, and $J/\psi \rightarrow \mu^+\mu^-$. These decays can be identified by peaks at the nominal D and J/ψ mass in the distributions of the invariant masses of two of the final-state particles ($M_{K^-\pi^+}$, $M_{\pi^+K_S^0}$, $M_{K^-K_S^0}$, and the cases with changing the masses hypothesis of charged kaon or pion). We exclude the events within $\pm 4\sigma$ of the peaking structures to suppress the contributions from D mesons and J/ψ .

The rare B background coming from $b \rightarrow u, d, s$ transitions is studied with a large MC sample in which the branching fractions are much larger than the measured or expected value. Two modes are found to have peaks near the ΔE signal region: $B^0 \rightarrow K^-K^+K_S^0$ and $B^0 \rightarrow \pi^-\pi^+K_S^0$, including their intermediate resonant modes. Rest of the rare B events

have a relatively flat ΔE distribution.

The signal yield and \mathcal{A} are extracted from a three-dimensional extended unbinned maximum likelihood fit, with the likelihood defined as

$$\mathcal{L} = \frac{e^{-\sum_j N_j}}{N!} \prod_{i=1}^N \left(\sum_j N_j P_j^i \right), \quad (2)$$

where,

$$P_j^i = \frac{1}{2}(1 - q^i \cdot \mathcal{A}_j) \times P_j(M_{bc}^i, \Delta E^i, C'_{NN}{}^i), \quad (3)$$

N is the total number of candidate events, N_j is the number of events in category j , i denotes event index, q^i is the charge of K^\pm in the i -th event, \mathcal{A}_j is the value of final-state asymmetry of the j -th category, P_j represents the value of the corresponding three-dimensional probability density function (PDF), and M_{bc}^i , ΔE^i , and $C'_{NN}{}^i$ are the M_{bc} , ΔE , and C'_{NN} value of the i -th event, respectively.

With all the selection criteria applied, the signal MC sample contains 98% of the correctly-reconstructed signal B events ('true' signal) and 2% self-crossfeed (scf) events. In the fit, the ratio of scf to true signal events is fixed. The signal yield (N_{sig}) is the combined yield of the two PDFs. In addition to the signal part, five more categories are included in the fit: continuum background, generic B background, $B^0 \rightarrow K^- K^+ K_S^0$, $B^0 \rightarrow \pi^- \pi^+ K_S^0$, and the rest of the rare B background. The true signal PDF is described by a product of a sum of two Gaussian functions in M_{bc} , a sum of three Gaussian functions in ΔE , and an asymmetric Gaussian function in C'_{NN} . These signal PDF shapes are calibrated including possible data-MC differences obtained from study of the control mode: $\bar{B}^0 \rightarrow D^- \pi^+$ with $D^- \rightarrow K_S^0 \pi^-$. The continuum background PDF is described by a product of an ARGUS function [25] in M_{bc} , a second-order polynomial in ΔE , and a combination of a Gaussian and an asymmetric Gaussian function in C'_{NN} . The shape parameters of the continuum background PDF are free in the data fit, except for the ARGUS end-point which is fixed to 5.2892 GeV/ c^2 . For the others (scf, generic B , $B^0 \rightarrow K^- K^+ K_S^0$, $B^0 \rightarrow \pi^- \pi^+ K_S^0$, and rare B), their PDFs are described by a smoothed histogram in ΔE and M_{bc} , and an asymmetric Gaussian function in C'_{NN} whose shape is based on MC. The yield of each category is floated. Except for the signal, \mathcal{A} is fixed to zero for the other categories.

The projections of the fit are shown in Fig. 1. We obtain a signal yield of 490_{-45}^{+46} with a statistical significance of 13 standard deviations, and an \mathcal{A} of $(-8.5 \pm 8.9)\%$. The significance is defined as $\sqrt{-2\ln(\mathcal{L}_0/\mathcal{L}_{\text{max}})}$, where \mathcal{L}_0 and \mathcal{L}_{max} are the likelihood values obtained by the fit with and without the signal yield fixed to zero, respectively.

The branching fraction is calculated using

$$\mathcal{B} = \frac{N_{\text{sig}}}{\epsilon \times \eta \times N_{B\bar{B}}}, \quad (4)$$

where N_{sig} , $N_{B\bar{B}}$, ϵ , and η are the fitted signal yield, the number of $B\bar{B}$ pairs ($= 772 \times 10^6$), the reconstruction efficiency of signal, and the efficiency calibration factor, respectively. The last quantity contains calibrations due to various systematic effects: $\eta = \eta_K \times \eta_\pi \times \eta_{NN} \times \eta_{\text{fit}}$, where $\eta_K (= 0.9948 \pm 0.0083)$ and $\eta_\pi (= 0.9512 \pm 0.0079)$ are the corrections due to the K^\pm and π^\pm identification with requirement on L_K and L_π , and are obtained by the control sample study of $D^{*+} \rightarrow D^0 \pi^+$ with $D^0 \rightarrow K^+ \pi^-$, $\eta_{NN} (= 0.9897 \pm 0.0208)$ is due to the requirement on C_{NN} and is obtained by the $B^0 \rightarrow D^- \pi^+$ with $D^- \rightarrow K_S^0 \pi^-$ control sample

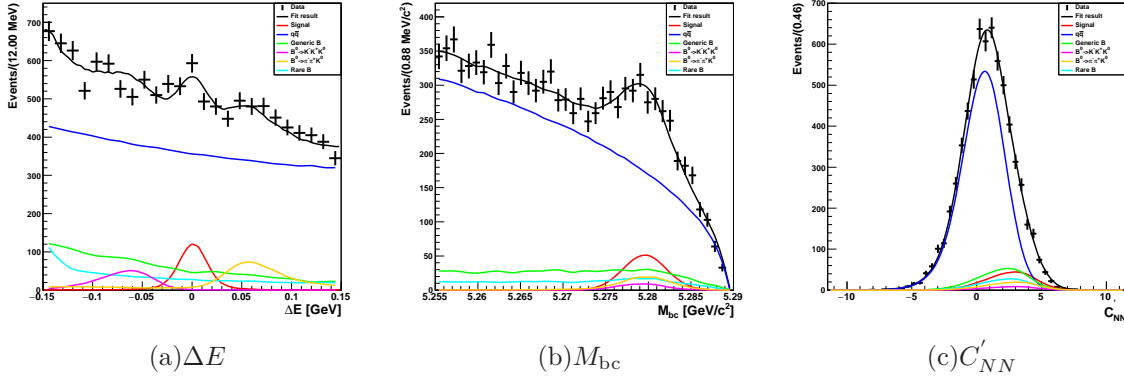


FIG. 1: Projections of the fit results of $\bar{B}^0(B^0) \rightarrow K_S^0 K^\mp \pi^\pm$ decay on ΔE , M_{bc} , and C'_{NN} . (a) ΔE in $5.272 \text{ GeV}/c^2 < M_{bc} < 5.288 \text{ GeV}/c^2$ and $0 < C'_{NN} < 5$. (b) M_{bc} in $|\Delta E| < 0.05 \text{ GeV}$ and $0 < C'_{NN} < 5$. (c) C'_{NN} in $|\Delta E| < 0.05 \text{ GeV}$ and $5.272 \text{ GeV}/c^2 < M_{bc} < 5.288 \text{ GeV}/c^2$.

study, and $\eta_{\text{fit}} (= 1.022 \pm 0.004)$ is due to fit bias and is obtained by ensemble test on the fitter. The reconstruction efficiency for the signal (ϵ) is $(26.7 \pm 0.03)\%$ with all the selection criteria applied.

Figure 2 shows the background-subtracted Dalitz plot obtained with the *sPlot* method. There seem to be some structures around the region of $2 \text{ GeV}^2/c^4 > M_{K-K_S^0}^2$ and $7 \text{ GeV}^2/c^4 < M_{\pi+K_S^0}^2 < 23 \text{ GeV}^2/c^4$. To check the projections on the Dalitz variables, we also obtain their background-subtracted distributions after separating them into five bins, and then calculate the differential branching fraction as function of the three Dalitz variables with the yield and reconstruction efficiency within each bin. Figure 3 shows the differential branching fraction as functions of the three Dalitz variables including comparison to the MC with a three-body phase space decay model. Large deviation from the phase space expectation is found at the second bin (around $1.2 \text{ GeV}/c^2$) of the $M_{K-K_S^0}$ spectrum and at the fifth bin (around $4.2 \text{ GeV}/c^2$) of the $M_{\pi+K_S^0}$ spectrum. In addition, no obvious structure is seen at both the low $M_{K-\pi^+}$ and $M_{\pi+K_S^0}$ regions, which are also consistent with the previous two-body decays' measurements of $B^0 \rightarrow K^{*\pm} K^\mp$ [7] and $B^0 \rightarrow \bar{K}^0 K^*(892)^0$ [5, 8].

To check the localized final-state asymmetry, differential branching fraction for the $K_S^0 K^- \pi^+$ and $K_S^0 K^+ \pi^-$ final states are shown in Fig. 4. Within each bin of the Dalitz variables, we see null asymmetry since there is no significant difference in the branching fractions between the two final states. The details of differential branching fraction calculation in each bin are summarized in Table I.

Sources of various systematic uncertainties on the branching fraction calculation are shown in Table II. The uncertainty due to the total number of $B\bar{B}$ pairs is 1.4%. The uncertainty due to the charged-track reconstruction efficiency is estimated to be 0.35% per track by using the partially reconstructed $D^{*+} \rightarrow D^0 \pi^+$ with $D^0 \rightarrow \pi^+ \pi^- K_S^0$ events. The uncertainty due to the K^\pm and π^\pm identification are obtained by the control sample study of $D^{*+} \rightarrow D^0 \pi^+$ with $D^0 \rightarrow K^+ \pi^-$. The uncertainty due to the $K_S^0 \rightarrow \pi^+ \pi^-$ branching fraction is based on the world average value $(69.2 \pm 0.05)\%$ [24]. The uncertainty due to K_S^0 identification is estimated to be 1.6% based on a control sample of $D^{*+} \rightarrow D^0 \pi^+$ with $D^0 \rightarrow K_S^0 \pi^0$. The uncertainty due to continuum suppression with the requirement on C_{NN} and is obtained by the $B^0 \rightarrow D^- \pi^+$ with $D^- \rightarrow K_S^0 \pi^-$ control sample study. The

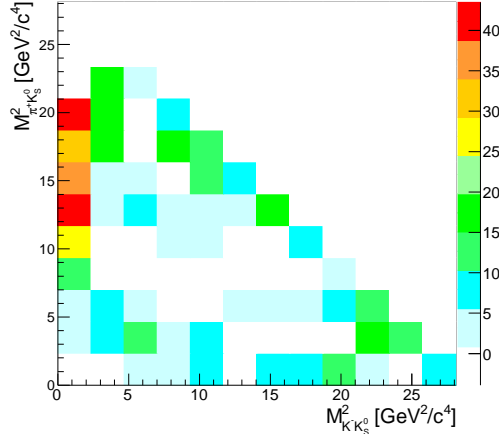


FIG. 2: Background-subtracted Dalitz plot of the $\bar{B}^0(B^0) \rightarrow K_S^0 K^\mp \pi^\pm$ decay.

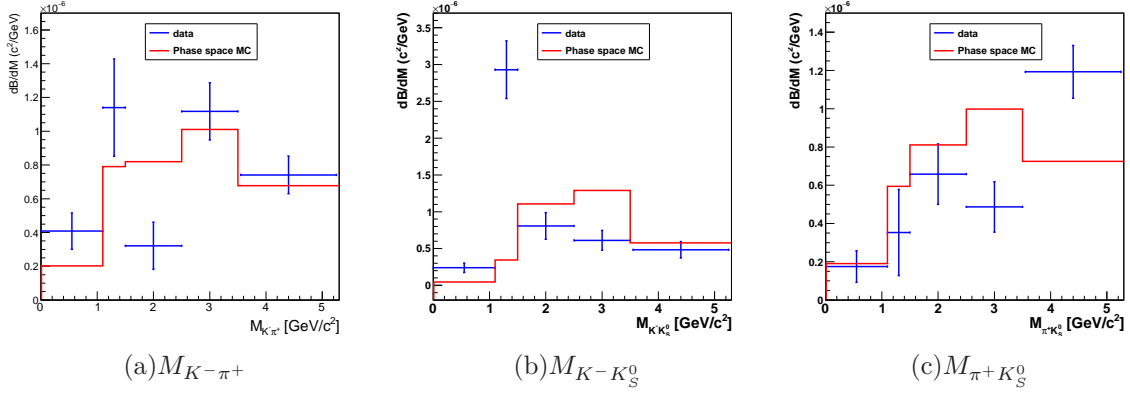


FIG. 3: Differential branching fraction as a function of $M_{K-\pi^+}$, $M_{K-K_S^0}$, and $M_{\pi+K_S^0}$. The blue error bar is the data result. The red error bar is obtained by using a signal MC sample with 3-body phase space decay model.

uncertainty of the reconstruction efficiency is estimated due to limited MC statistics. The uncertainty due to the fixed signal and background PDF shapes is estimated by the deviation of fitted signal yield with varying the conditions of those PDFs in different cases. For all the smoothed histograms, we vary the binning conditions of those histograms. For the other PDFs with fixed parameterization, the fixed parameters are randomized by using Gaussian random number to repeat data fits with various parameter sets, and the uncertainty of the yield distribution is quoted. The uncertainty due to fit bias is obtained by ensemble test on the fitter.

Sources of various systematic uncertainties on \mathcal{A} are listed in Table III. The uncertainty due to K^\pm and π^\pm detection bias are obtained by control sample studies of $D^+ \rightarrow \phi\pi^+$ and $D_s^+ \rightarrow \phi\pi^+$ [26], and $D^+ \rightarrow K_S^0\pi^+$ [27], respectively. The uncertainty due to the fixed signal and background PDF shapes is using the same way as the one for the uncertainty on branching fraction. It is also estimated by the deviation of fitted \mathcal{A} with varying the conditions of those PDFs in different cases.

In conclusion, we have performed a measurement of branching fraction and \mathcal{A} of the

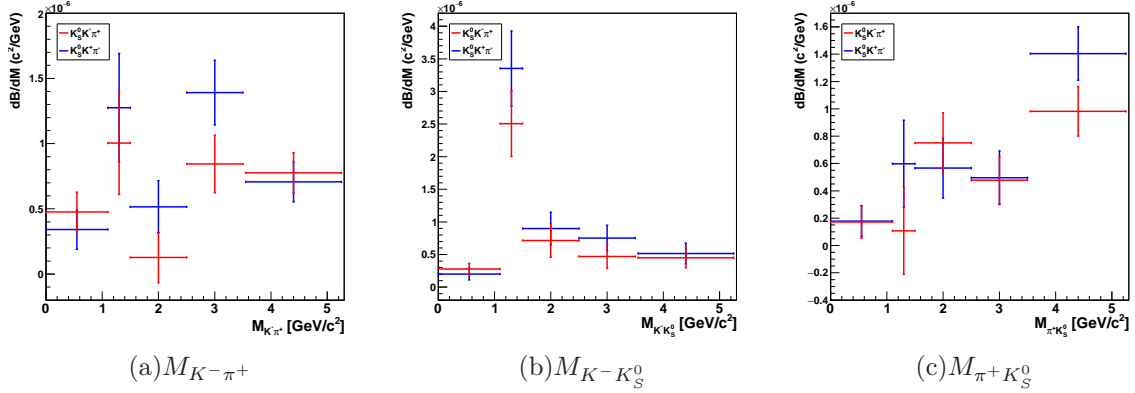


FIG. 4: Differential branching fraction as functions of the $M_{K^- \pi^+}$, $M_{K^- K_S^0}$, and $M_{\pi^+ K_S^0}$ for the two reconstructed B final states: $K_S^0 K^- \pi^+$ (red error bar) and $K_S^0 K^+ \pi^-$ (blue error bar).

TABLE I: Signal yields, efficiency, and differential branching fraction in each $M_{K^- \pi^+}$, $M_{K^- K_S^0}$, and $M_{\pi^+ K_S^0}$ bin.

(GeV/c ²)	eff.	Yield	$d\mathcal{B}/dM$ (10^{-7})	$K_S^0 K^- \pi^+$ yield	$K_S^0 K^+ \pi^-$ yield	$K_S^0 K^- \pi^+$ $d\mathcal{B}/dM$ (10^{-7})	$K_S^0 K^+ \pi^-$ $d\mathcal{B}/dM$ (10^{-7})
$M_{K^- \pi^+}$							
0~1.1	0.301	$69.2 \pm 18.0 \pm 3.0$	$4.1 \pm 1.1 \pm 0.2$	$40.3 \pm 12.7 \pm 1.7$	$28.9 \pm 12.8 \pm 1.2$	$4.5 \pm 1.5 \pm 0.2$	$3.4 \pm 1.5 \pm 0.1$
1.1~1.5	0.306	$71.3 \pm 17.8 \pm 3.1$	$11.4 \pm 2.8 \pm 0.5$	$31.4 \pm 12.3 \pm 1.4$	$39.9 \pm 12.9 \pm 1.7$	$10.0 \pm 3.9 \pm 0.4$	$12.8 \pm 4.1 \pm 0.5$
1.5~2.5	0.289	$47.5 \pm 20.5 \pm 2.0$	$3.2 \pm 1.4 \pm 0.1$	$9.4 \pm 14.3 \pm 0.4$	$38.1 \pm 14.7 \pm 1.6$	$1.3 \pm 1.9 \pm 0.1$	$5.2 \pm 2.0 \pm 0.2$
2.5~3.5	0.262	$149.7 \pm 21.7 \pm 6.4$	$11.2 \pm 1.6 \pm 0.5$	$56.5 \pm 14.6 \pm 2.4$	$93.2 \pm 16.1 \pm 4.0$	$8.4 \pm 2.2 \pm 0.4$	$13.9 \pm 2.4 \pm 0.6$
>3.5	0.237	$152.7 \pm 22.0 \pm 6.6$	$7.4 \pm 1.1 \pm 0.3$	$79.9 \pm 15.5 \pm 3.4$	$72.8 \pm 15.5 \pm 3.1$	$7.8 \pm 1.5 \pm 0.3$	$7.1 \pm 1.5 \pm 0.3$
$M_{\pi^+ K_S^0}$							
0~1.1	0.275	$27.1 \pm 12.7 \pm 1.2$	$1.8 \pm 0.8 \pm 0.1$	$13.3 \pm 9.2 \pm 0.6$	$13.8 \pm 8.7 \pm 0.6$	$1.7 \pm 1.2 \pm 0.1$	$1.8 \pm 1.1 \pm 0.1$
1.1~1.5	0.269	$19.4 \pm 12.4 \pm 0.8$	$3.5 \pm 2.2 \pm 0.2$	$3.0 \pm 8.8 \pm 0.1$	$16.5 \pm 8.7 \pm 0.7$	$1.1 \pm 3.2 \pm 0.0$	$6.0 \pm 3.2 \pm 0.3$
1.5~2.5	0.252	$84.8 \pm 20.0 \pm 3.6$	$6.6 \pm 1.5 \pm 0.3$	$48.3 \pm 14.2 \pm 2.1$	$36.5 \pm 14.1 \pm 1.6$	$7.5 \pm 2.2 \pm 0.3$	$5.7 \pm 2.2 \pm 0.2$
2.5~3.5	0.264	$65.7 \pm 17.6 \pm 2.8$	$4.9 \pm 1.3 \pm 0.2$	$32.2 \pm 11.7 \pm 1.4$	$33.4 \pm 13.2 \pm 1.4$	$4.8 \pm 1.7 \pm 0.2$	$5.0 \pm 1.9 \pm 0.2$
>3.5	0.283	$293.4 \pm 31.5 \pm 12.6$	$11.9 \pm 1.3 \pm 0.5$	$120.7 \pm 21.7 \pm 5.2$	$172.7 \pm 22.8 \pm 7.4$	$9.8 \pm 1.8 \pm 0.4$	$14.0 \pm 1.9 \pm 0.6$
$M_{K^- K_S^0}$							
0~1.1	0.245	$32.9 \pm 8.5 \pm 1.4$	$2.4 \pm 0.6 \pm 0.1$	$19.1 \pm 5.8 \pm 0.8$	$13.7 \pm 6.2 \pm 0.6$	$2.8 \pm 0.8 \pm 0.1$	$2.0 \pm 0.9 \pm 0.1$
1.1~1.5	0.258	$154.6 \pm 19.6 \pm 6.6$	$29.3 \pm 3.7 \pm 1.3$	$66.1 \pm 13.0 \pm 2.8$	$88.5 \pm 14.7 \pm 3.8$	$25.1 \pm 4.9 \pm 1.1$	$33.5 \pm 5.6 \pm 1.4$
1.5~2.5	0.235	$96.9 \pm 21.3 \pm 4.2$	$8.1 \pm 1.8 \pm 0.3$	$43.0 \pm 15.3 \pm 1.8$	$53.9 \pm 14.8 \pm 2.3$	$7.2 \pm 2.6 \pm 0.3$	$9.0 \pm 2.5 \pm 0.4$
2.5~3.5	0.267	$83.4 \pm 18.1 \pm 3.6$	$6.1 \pm 1.3 \pm 0.3$	$32.1 \pm 12.3 \pm 1.4$	$51.3 \pm 13.2 \pm 2.2$	$4.7 \pm 1.8 \pm 0.2$	$7.5 \pm 1.9 \pm 0.3$
>3.5	0.292	$122.6 \pm 27.8 \pm 5.3$	$4.8 \pm 1.1 \pm 0.2$	$57.2 \pm 19.5 \pm 2.5$	$65.5 \pm 19.9 \pm 2.8$	$4.5 \pm 1.5 \pm 0.2$	$5.2 \pm 1.6 \pm 0.2$

$\bar{B}^0(B^0) \rightarrow K_S^0 K^\mp \pi^\pm$ decay based on a data sample of 711 fb^{-1} collected by Belle. We obtain a branching fraction of $(3.60 \pm 0.33 \pm 0.15) \times 10^{-6}$ and an \mathcal{A} of $(-8.5 \pm 8.9 \pm 0.2)\%$, where their first uncertainty is statistical and the second is systematic. The measured \mathcal{A} is consistent with null asymmetry. Hints of peaking structures are seen around a region of $2 \text{ GeV}^2/c^4 > M_{K^- K_S^0}^2$ and $7 \text{ GeV}^2/c^4 < M_{\pi^+ K_S^0}^2 < 23 \text{ GeV}^2/c^4$ in the Dalitz plot. A cross-check is done by the differential branching fraction with projecting on each Dalitz variable, and hints of peaking resonances are seen at around $1.2 \text{ GeV}/c^2$ of $M_{K^- K_S^0}$ and around $4.2 \text{ GeV}/c^2$ of $M_{\pi^+ K_S^0}$ when compared to the phase space MC. No obvious K^* structure is seen at both the low $M_{K^- \pi^+}$ and $M_{\pi^+ K_S^0}$ spectrum, which is also consistent with the BaBar and LHCb results [5, 7, 8]. No localized final-state asymmetry is observed. In the near

TABLE II: Summary of systematic uncertainties on the branching fraction.

Source	in %
$N_{B\bar{B}}$	1.4
Tracking	0.7
K^\pm identification	0.8
π^\pm identification	0.8
$\mathcal{B}(K_S^0 \rightarrow \pi^+\pi^-)$	0.1
$K_S^0 \rightarrow \pi^+\pi^-$ identification	1.6
Continuum suppression with NN	2.1
Reconstruction efficiency (MC statistics)	0.1
Signal PDF	2.7
Background PDF	0.4
Fit bias	0.4
Total	4.3

TABLE III: Summary of systematic uncertainties on \mathcal{A} .

Source	in %
Detector bias	0.6
Signal PDF	2.7
Background PDF	0.9
Total	2.9

future, the experiments with large data sets such as Belle II and LHCb can provide more detailed analysis employing a full Dalitz analysis to search for the intermediate resonances and localized final-state asymmetry.

We thank the KEKB group for the excellent operation of the accelerator; the KEK cryogenics group for the efficient operation of the solenoid; and the KEK computer group, the National Institute of Informatics, and the PNNL/EMSL computing group for valuable computing and SINET4 network support. We acknowledge support from the Ministry of Education, Culture, Sports, Science, and Technology (MEXT) of Japan, the Japan Society for the Promotion of Science (JSPS), and the Tau-Lepton Physics Research Center of Nagoya University; the Australian Research Council; Austrian Science Fund under Grant No. P 22742-N16 and P 26794-N20; the National Natural Science Foundation of China under Contracts No. 10575109, No. 10775142, No. 10875115, No. 11175187, No. 11475187 and No. 11575017; the Chinese Academy of Science Center for Excellence in Particle Physics; the Ministry of Education, Youth and Sports of the Czech Republic under Contract No. LG14034; the Carl Zeiss Foundation, the Deutsche Forschungsgemeinschaft, the Excellence Cluster Universe, and the VolkswagenStiftung; the Department of Science and Technology of India; the Istituto Nazionale di Fisica Nucleare of Italy; the WCU program of the Ministry of Education, National Research Foundation (NRF) of Korea Grants No. 2011-0029457, No. 2012-

0008143, No. 2012R1A1A2008330, No. 2013R1A1A3007772, No. 2014R1A2A2A01005286, No. 2014R1A2A2A01002734, No. 2015R1A2A2A01003280, No. 2015H1A2A1033649; the Basic Research Lab program under NRF Grant No. KRF-2011-0020333, Center for Korean J-PARC Users, No. NRF-2013K1A3A7A06056592; the Brain Korea 21-Plus program and Radiation Science Research Institute; the Polish Ministry of Science and Higher Education and the National Science Center; the Ministry of Education and Science of the Russian Federation and the Russian Foundation for Basic Research; the Slovenian Research Agency; Ikerbasque, Basque Foundation for Science and the Euskal Herriko Unibertsitatea (UPV/EHU) under program UFI 11/55 (Spain); the Swiss National Science Foundation; the Ministry of Education and the Ministry of Science and Technology of Taiwan; and the U.S. Department of Energy and the National Science Foundation. This work is supported by a Grant-in-Aid from MEXT for Science Research in a Priority Area (“New Development of Flavor Physics”) and from JSPS for Creative Scientific Research (“Evolution of Tau-lepton Physics”).

-
- [1] I. Bediaga *et al.*, Phys. Rev. D **80**, 096006 (2009).
[2] I. Bediaga *et al.*, Phys. Rev. D **86**, 036005 (2012).
[3] Throughout this paper, inclusion of charge-conjugate decay modes is always implied.
[4] P. del Amo Sanchez *et al.*, (BABAR Collaboration) Phys. Rev. D **82**, 031101 (2010).
[5] B. Aubert *et al.*, (BABAR Collaboration) Phys. Rev. D **74**, 072008 (2016).
[6] Aaij, R., Adeva, B. *et al.*, (LHCb Collaboration) J. High Energy Phys. 11 (2017) 027
[7] Aaij, R., Adeva, B. *et al.*, (LHCb Collaboration) New Journal of Physics. 16 (2014) 123001
[8] Aaij, R., Adeva, B. *et al.*, (LHCb Collaboration) J. High Energy Phys. 01 (2016) 012
[9] C.-L. Hsu *et al.*, (Belle Collaboration) Phys. Rev. D **96**, 031101 (2017).
[10] B. Aubert *et al.*, (BABAR Collaboration) Phys. Rev. Lett. **99**, 221801 (2007).
[11] R. Aaij *et al.*, (LHCb Collaboration) Phys. Rev. Lett. **112**, 011801 (2014).
[12] R. Aaij *et al.*, (LHCb Collaboration) Phys. Rev. D **90**, 112004 (2014).
[13] M. Pivk and F R. Le Diberder, arXiv:physics/0402083.
[14] A. Abashian *et al.* (Belle Collaboration), Nucl. Instrum. Methods Phys. Res. Sect. A **479**, 117 (2002); also see detector section in J. Brodzicka *et al.*, Prog. Theor. Exp. Phys. (2012) 04D001.
[15] S. Kurokawa and E. Kikutani, Nucl. Instrum. Methods Phys. Res. Sect. A **499**, 1 (2003), and other papers included in this Volume; T.Abe *et al.*, Prog. Theor. Exp. Phys. **2013**, 03A001 (2013) and references therein.
[16] Z. Natkaniec *et al.* (Belle SVD2 Group), Nucl. Instrum. Methods Phys. Res. Sect. A **560**, 1 (2006).
[17] D. J. Lange *et al.*, Nucl. Instrum. Methods Phys. Res. Sect. A **462**, 152 (2001).
[18] R. Brun *et al.*, GEANT 3.21, CERN Report No. DD/EE/84-1 (1987).
[19] M. Feindt and U. Kerzel, Nucl. Instrum. and Methods in Phys. Res., Sect. A **559** 190 (2006).
[20] N. Dash *et al.* (Belle Collaboration), Phys. Rev. Lett. **119**, 171801 (2017).
[21] R. A. Fisher, Annals of Human Genetics **7**, 179 (1936); also available at <http://dx.doi.org/10.1111/j.1469-1809.1936.tb02137.x>
[22] G.C. Fox and S. Wolfram, Phys. Rev. Lett. **41**, 1581 (1978). The modified moments used in this paper are described in, S.H. Lee *et al.* (Belle Collab.), Phys. Rev. Lett. **91**, 261801 (2003).

- [23] S. Brandt, C. Peyrou, R. Sosnowski, and A. Wroblewski, *Phys. Lett.* **12**, 57 (1964).
- [24] M. Tanabashi *et al.* (Particle Data Group), *Phys. Rev. D* **98**, 010001 (2018).
- [25] H. Albrecht *et al.* (ARGUS Collaboration), *Phys. Lett. B* **241**, 278 (1990).
- [26] M. Starič *et al.* (Belle Collaboration), *Phys. Rev. Lett.* **108**, 071801 (2012).
- [27] B. R. Ko *et al.* (Belle Collaboration), *Phys. Rev. Lett.* **109**, 021601 (2012).